# Single-Molecule Cut-and-Paste Surface Assembly

S. K. Kufer, *et al.*

*Science* **319**, 594 (2008);
DOI: 10.1126/science.1151424



*Science* (print ISSN 0036-8075; online ISSN 1095-9203) is published weekly, except the last week in December, by the American Association for the Advancement of Science, 1200 New York Avenue NW, Washington, DC 20005. 

19. V. Reinke, I. S. Gil, S. Ward, K. Kazmer, *Development* **131**, 311 (2004).
20. H. Browning, S. Strome, *Development* **122**, 391 (1996).
21. R. W. Beeman, K. S. Friesen, R. E. Denell, *Science* **256**, 89 (1992).
22. G. D. Hurst, J. H. Werren, *Nat. Rev. Genet.* **2**, 597 (2001).
23. A. Atlan, H. Mercot, C. Landre, C. Montchamp-Moreau, *Evol. Int. J. Org. Evol.* **51**, 1886 (1997).
24. R. W. Beeman, K. S. Friesen, *Heredity* **82**, 529 (1999).
25. L. Fishman, J. H. Willis, *Genetics* **169**, 347 (2005).
26. H. A. Orr, S. Irving, *Genetics* **169**, 671 (2005).
27. F. A. Reed, R. G. Reeves, C. F. Aquadro, *Evol. Int. J. Org. Evol.* **59**, 1280 (2005).
28. E. A. Stahl, G. Dwyer, R. Mauricio, M. Kreitman, J. Bergelson, *Nature* **400**, 667 (1999).
29. D. Tian, H. Araki, E. Stahl, J. Bergelson, M. Kreitman, *Proc. Natl. Acad. Sci. U.S.A.* **99**, 11525 (2002).
30. M. Shapira *et al*., *Proc. Natl. Acad. Sci. U.S.A.* **103**, 14086 (2006).
31. J. H. Thomas, *Genome Res.* **16**, 1017 (2006).
32. J. H. Thomas, *Genetics* **172**, 127 (2006).
33. H. A. Orr, D. C. Presgraves, *Bioessays* **22**, 1085 (2000).
34. K. A. Frazer, L. Pachter, A. Poliakov, E. M. Rubin, I. Dubchak, *Nucleic Acids Res.* **32**, W273 (2004).
35. Z. Yang, *Comput. Appl. Biosci.* **13**, 555 (1997).
36. We thank the *Caenorhabditis* Genetics Center, the National Bioresource Project of Japan, the NemaGENETAG Consortium, M.-A. Félix, A. Barrière, E. Dolgin, and H. Van Epps for strains; R. Maruyama and A. Singson for advice; S. Skrovanek for lab assistance; and H. Coller, A. Cutter, D. Gresham, R. Gosh, L. Moyle, J. Shapiro, and E. Smith for comments on the manuscript. Supported by a National Defense Science and Engineering Graduate fellowship to H.S.S., a Jane Coffin Childs Fellowship to M.V.R., NIH grants R37 MH059520 and R01 HG004321 and a James S. McDonnell Foundation Centennial Fellowship to L.K., and NIH grant GM071508 to the Lewis-Sigler Institute. GenBank sequence accession numbers are EU163897 to EU163940.

**Supporting Online Material**

www.sciencemag.org/cgi/content/full/1151107/DC1
SOM Text
Fig. S1
Tables S1 to S7
References

28 September 2007; accepted 17 December 2007
Published online 10 January 2008;
10.1126/science.1151107
Include this information when citing this paper.

REPORTS

# Single-Molecule Cut-and-Paste Surface Assembly

**S. K. Kufer,[1] E. M. Puchner,[1] H. Gumpp,[1] T. Liedl,[2] H. E. Gaub[1]**

**We introduce a method for the bottom-up assembly of biomolecular structures that combines the precision of the atomic force microscope (AFM) with the selectivity of DNA hybridization. Functional units coupled to DNA oligomers were picked up from a depot area by means of a complementary DNA strand bound to an AFM tip. These units were transferred to and deposited on a target area to create basic geometrical structures, assembled from units with different functions. Each of these cut-and-paste events was characterized by single-molecule force spectroscopy and single-molecule fluorescence microscopy. Transport and deposition of more than 5000 units were achieved, with less than 10% loss in transfer efficiency.**

Functional biomolecular assembly aims to create structures from a large variety of biomolecular building blocks in a geometrically well-defined manner in order to create new functions (*1*, *2*), such as artificial signaling cascades or synergetic combinations of enzymes. Hybrid devices could include quantum dots coassembled with dye molecules, or gold particles assembled as plasmon hot spots with a sample protein positioned into the focus (*3*). One way to assemble such molecular devices would be to physically pick up the different units needed with a scanning probe tip, translocate these units to a different location, and deposit them with high spatial precision (*4*–*6*). The entire process would also have to be carried out in an aqueous environment.

For the translocation of nanoscale objects, we used atomic force microscopy, which has been used in this context for mechanical single-molecule experiments (*7*–*12*) or lithography (*13*, *14*); however, previously suggested devices include the use of molecular pliers at the end of atomic force microscope (AFM) cantilevers that could grab and release the building blocks, triggered by an external signal of either electrical or optical nature (*15*). We report a simpler and robust solution based on DNA hybridization and hierarchical bonds defined by different unbinding forces.

A well-sorted "depot," with a large variety of molecular species, stably stored in well-defined loci, is a prerequisite for the assembly of a multicomponent device. DNA chips offer a freely programmable pattern of oligomers that are commercially available and have spot sizes in the submicrometer range (*16*). Niemeyer *et al*. (*17*) converted such a DNA pattern into a protein pattern by binding a DNA-labeled protein to its corresponding spot on a DNA chip. The length of the oligomers can be chosen so that after incubation and stringent washing, a thermodynamically stable pattern of proteins is obtained. Given the known sequence map of the DNA chip, different molecular species can be stored in a known position on the depot chip. Alternatively, when only a limited variety of building blocks is needed, microfluidic elastomer channels may be used to create patterns (*18*–*20*) of building blocks, which after removal of the elastomer may be manipulated with the AFM tip (fig. S3).

We used this approach to store our functional units and also extended the DNA oligomers to fulfill a second function; namely, to serve as a handle (Fig. 1). This additional stretch of DNA can hybridize to a complementary DNA covalently attached to an AFM tip. We chose the duplexes to be comparable in length and binding free energy, but we selected the sequences so that the anchor hybridizes in the so-called "unzip" geometry and the handle hybridizes in the "shear" geometry [Fig. 1 and (*21*)]. These two duplex geometries differ substantially in that, upon forced unbinding, the zipper duplex is opened up base pair by base pair, whereas in the shear geometry, all base pairs are loaded in parallel (Fig. 2 and fig. S1). Although the thermodynamic stability and the spontaneous off rate of both geometries are comparable, their rupture forces differ dramatically (*22*), as has been shown experimentally and was validated theoretically in several studies (*21*, *23*–*27*). Thus, upon retraction of the AFM tip, the anchor duplex will break open and the functional unit will be bound to the tip.

As can be seen in Fig. 2C, these force distance curves provide a characteristic fingerprint and serve as a robust criterion to decide whether a molecule was picked up from the depot. To avoid multiple transfers, we chose the density of the anchors on the tip to be low enough that in 35% of the attempts, only one unit was picked up, and in 20% of the attempts, just two units. In 20% of all attempts, we recorded traces like the lower two in Fig. 2C, which showed that we had not picked up any unit (fig. S5D). Because we recorded such a force distance curve for every pickup, we knew exactly how many units were transferred to the tip. The pickup process can be corrected online by either picking up more units or by dropping excess units in a "trash can" on the target area.

Once a unit is transferred to the tip, it can be moved to its new position on the target area. The target area had surface chemistry similar to that of the depot area, but the anchor oligomers were chosen so that when the tip was lowered, they bound to the transfer DNA in shear geometry and formed a duplex, which was longer than the handle duplex. Although the AFM tip can be positioned with subnanometer reproducibility, the precision with which the units can be

[1]Center for Nanoscience and Department of Physics, University of Munich, Amalienstrasse 54, 80799 Munich, Germany. [2]Department of Biological Chemistry and Molecular Pharmacology, Harvard Medical School, and Department of Cancer Biology, Dana-Farber Cancer Institute, Boston, MA 02115, USA.

deposited is limited by the lateral density of the anchor oligomers and their spacer length (presently in the 10-nm range).

Upon retraction of the tip from the surface, the force in the two DNA duplexes in series gradually increases until the weaker of the two complexes ruptures. The upper traces in Fig. 2D show examples of this process, which differs considerably in its signature from the unzipping shown in Fig. 2C (*28*, *29*). It was shown (*21*) that a length difference of 10 base pairs (bp) is sufficient to make the rupture of the shorter handle duplex more likely by one order of magnitude than the rupture of the longer anchor duplex. As was the case during pickup, no bond rupture was detected in certain cases (Fig. 2D, lower traces). Here the hybridization with the target anchor oligomer had failed, although a functional unit was offered. In the majority of cases, a second or third attempt made a few nanometers away from the originally planned target spot was successful. Again, a protocol with a characteristic force distance curve (for brevity referred to as a transfer protocol) was recorded for each transfer event. After delivery of the functional unit to the target, the oligomer covalently attached to the AFM tip was free again to hybridize with another handle sequence in the depot area.

For simplicity, we transferred only functional units of the same species but created patterns from single units with multiple functions instead. As functional units, we used molecular constructs consisting of a fluorophore (rhodamine green), a generic small ligand (biotin), and a DNA with extra overlap (which allows further docking of other units to the assembly in a later step) (Fig. 2 shows the schematics). The units were picked up

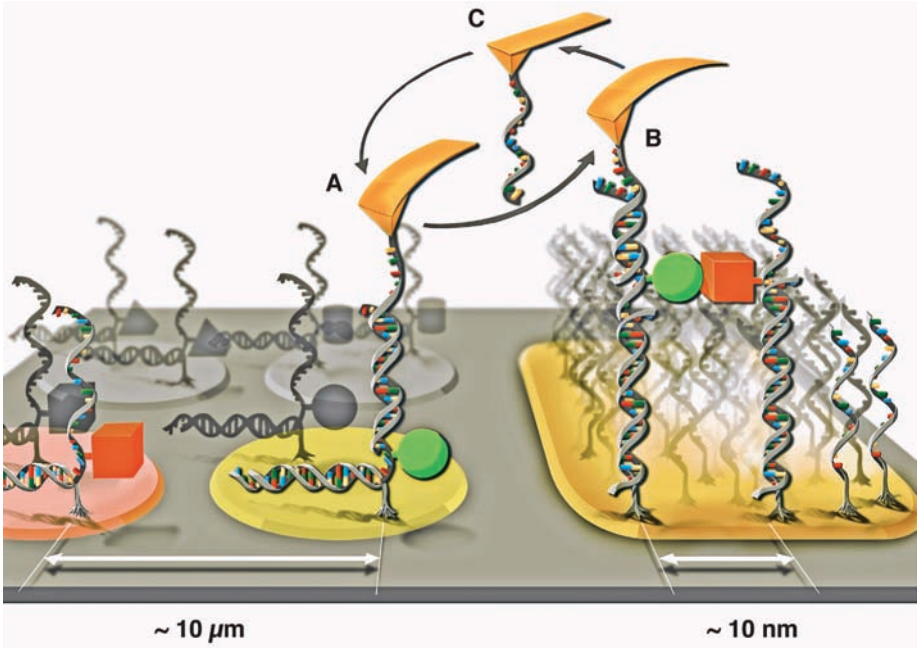


**Fig. 1.** Cartoon of the single-molecule cut-and-paste process. (**A**) Individual nanosized objects are picked up from discrete storage sites with a DNA oligomer at the tip of an AFM cantilever and transferred to a target site, where they are deposited with high spatial precision (**B**). (**C**) The length and binding geometry of the oligomers, which are used as an anchor or a handle, are chosen so that a hierarchy of unbinding forces allows the repetition of this process over and over again.

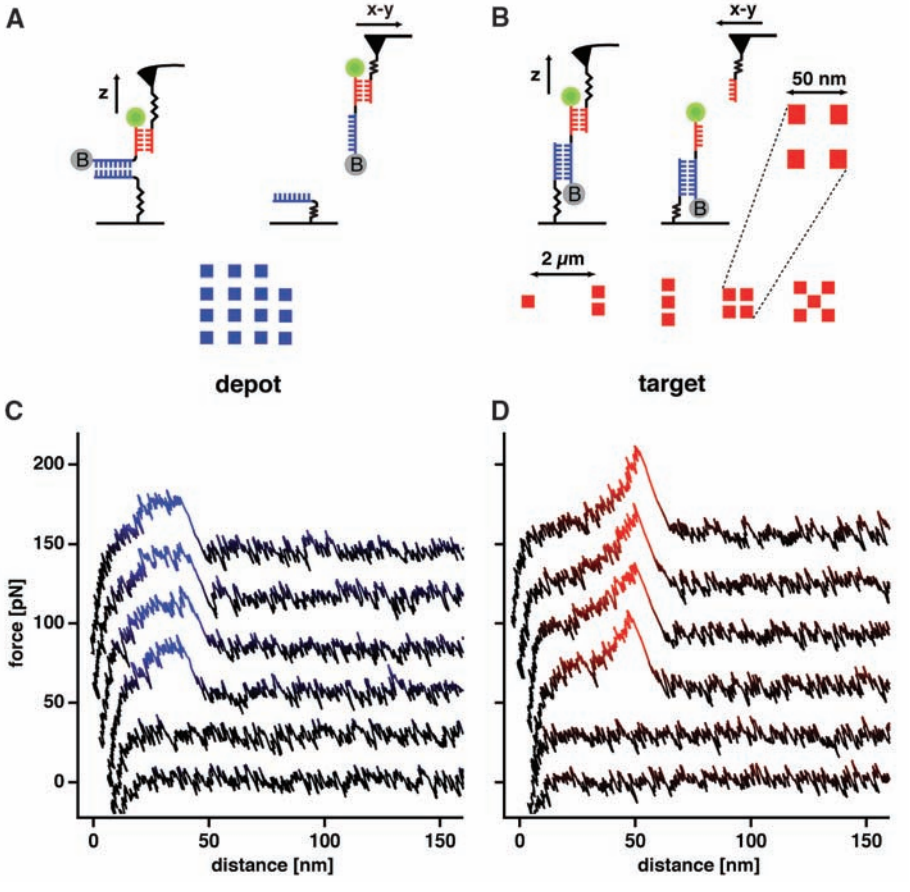


**Fig. 2.** Design of the assembled pattern with typical transfer protocols. (**A**) Individual functional units stored on the depot were picked up one at a time and transferred to the target area. The functional units consisted of a DNA oligomer with anchor and handle sequences, one fluorophore, one biotin, and an additional DNA binding site. (**B**) Five different patterns with different geometries were assembled on spots, which were 2 μm apart. In the first spot, we deposited one unit; in the second spot, two units with a lateral spacing of 50 nm; in the third spot, three units, and so forth. The lateral precision of the closed-loop feedback was ±6 nm. Force distance curves were recorded in every cycle as transfer protocols recording successful pickup and deposition. (**C**) Typical force distance curves measured during the pickup of functional units from the depot. At low extensions, the cantilever acts against the entropic force of the polyethylene glycol–DNA complex. When the force reaches about 20 pN, the anchor sequence is pulled open in a zipperlike mode, resulting in a plateau ~20 nm long. (**D**) Typical force distance curves recorded during the deposition of a single unit to the target area. The shape, with its sudden drop in force at about 50 pN, is characteristic of a rupture of a 20-bp DNA handle duplex loaded in shear geometry. The lower two force distance curves in (C) and (D) show attempts, where no transfer had occurred.

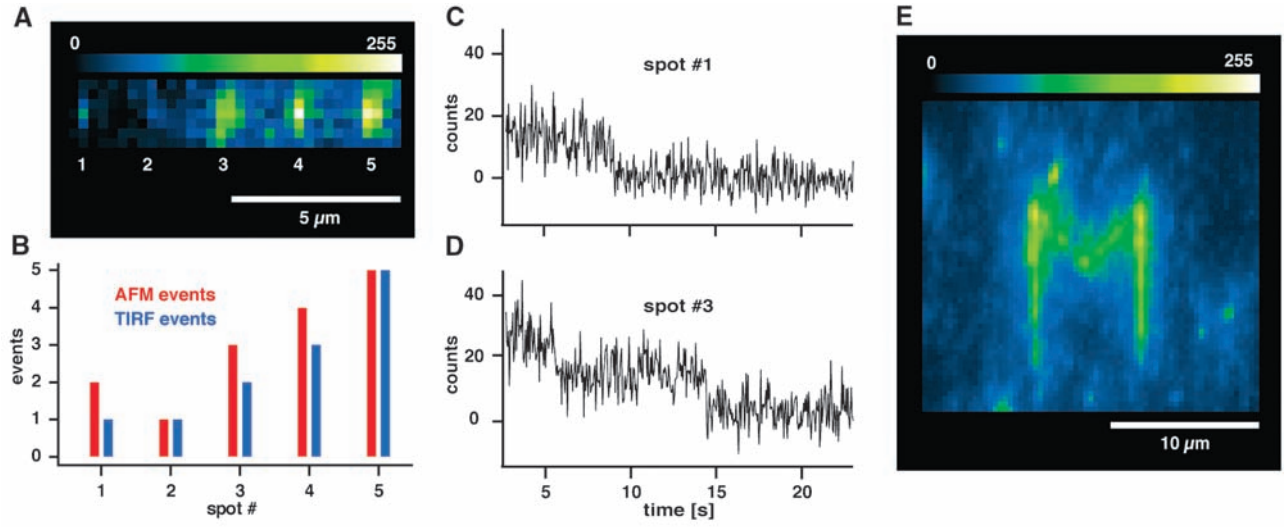


**Fig. 3.** (**A**) Fluorescence micrograph of the assembled pattern described in Fig. 2, imaged with TIRF excitation. The image was averaged over 440 frames, with 50 ms of integration time each. Because of the diffraction limit, individual fluorophores cannot be resolved spatially but can be resolved temporally. (**C**) and (**D**) show time traces of the two diffraction-limited 3 × 3–pixel–sized spots 1 and 3, exhibiting the typical stepwise bleaching of one and two single fluorophores, respectively. (**B**) Correlation analysis of the number of successfully transferred units as judged by the AFM transfer protocols and the number of bleaching steps in the fluorescence. (**E**) The capital letter M written by transporting 400 molecules from the depot area to defined positions at the target area. It was assembled with a tip that had already been used to transport more than 5000 molecules from the depot to the target area. These results demonstrate the long-term stability of the tip functionalization and the possibility of assembling extended constructs.

from a 100-nm-square pattern (Fig. 2A) and transferred to the target area. A pattern, as sketched in Fig. 2B, was assembled where we deposited a single unit in the first spot, a pair in the second spot, a triplet in the third, and so on. The transfer protocols always documented the actual number of transferred units.

After the assembly was completed, total internal reflection fluorescence (TIRF) imaging (*30*) showed discrete spots at the predicted positions (Fig. 3A). Because of the limited optical resolution, no details of the assemblies are resolved, but larger assemblies appear brighter. Time traces (Fig. 3, C and D) exhibited well-pronounced steps that were a clear indication of bleaching of individual fluorophores (*31*, *32*) (movie S1). On the spot in the first column, we recorded a single step only, and the fluorophore was bleached after 9 s. The spot in the third column exhibited only two steps, although our transfer protocol reported the deposition of three functional units. Either one of the fluorophores was inactive from the beginning or it was bleached during the first 2 s of the illumination and not recorded because of background fluorescence. A direct correlation between the number of deposited units as judged by the transfer protocol and the number of bleaching steps is given in Fig. 3B. Both independent experiments are in excellent agreement, which indicates that we lost only a minor fraction of fluorophores in the transfer process.

In order to demonstrate the formation of larger constructs, we assembled the capital letter M shown in Fig. 3E. It consists of 400 units and was written with a tip that had already been used to transport more than 5000 functional units from the depot to the target area. All of the data shown here and in the supporting online material were recorded with one cantilever. Because the pickup probability dropped by only 10% toward the end of the experiment, the lifetime of the tip functionalization was adequate. The pattern was assembled at an average rate of 7 s per transfer. This slow transfer rate was limited by the rather large distance between depot and target area of 15 μm and the closed-loop feedback of the translational stages of the instrument. The online analysis of the transfer protocols was also not optimized. The physical limits are given by the resonance frequency of the piezo stage, and so improvements of several orders of magnitude are possible (*33*). With the development of massively parallel–operating AFM cantilevers (*34*), molecule-by-molecule assembly based on hierarchical forces may evolve into a versatile technology.

### References and Notes


1. B. A. Grzybowski, H. A. Stone, G. M. Whitesides, *Nature* **405**, 1033 (2000).
2. T. Pellegrino *et al.*, *Small* **1**, 48 (2005).
3. M. Ringler *et al.*, *Nano Lett.* **7**, 2753 (2007).
4. D. M. Egler, E. K. Schweizer, *Nature* **344**, 524 (1990).
5. M. T. Cuberes, R. R. Schlittler, J. K. Gimzewski, *Appl. Phys. Lett.* **69**, 3016 (1996).
6. S. J. Greissl *et al.*, *J. Phys. Chem. B* **108**, 11556 (2004).
7. G. Binnig, H. Rohrer, C. Gerber, E. Weibel, *Phys. Rev. Lett.* **49**, 57 (1982).
8. G. Binnig, C. F. Quate, C. Gerber, *Phys. Rev. Lett.* **56**, 930 (1986).
9. P. K. Hansma, V. B. Elings, O. Marti, C. E. Bracker, *Science* **242**, 209 (1988).
10. M. Radmacher, R. W. Tillmann, M. Fritz, H. E. Gaub, *Science* **257**, 1900 (1992).
11. P. E. Marszalek *et al.*, *Nature* **402**, 100 (1999).
12. D. Fotiadis *et al.*, *Curr. Opin. Struct. Biol.* **16**, 252 (2006).
13. M. Jaschke *et al.*, *Biosens. Bioelectron.* **11**, 601 (1996).
14. R. D. Piner, J. Zhu, F. Xu, S. Hong, C. A. Mirkin, *Science* **283**, 661 (1999).
15. C. P. Collier *et al.*, *Science* **289**, 1172 (2000).
16. S. P. Fodor *et al.*, *Science* **251**, 767 (1991).
17. C. M. Niemeyer, T. Sano, C. L. Smith, C. R. Cantor, *Nucleic Acids Res.* **22**, 5530 (1994).
18. E. Delamarche, A. Bernard, H. Schmid, B. Michel, H. Biebuyck, *Science* **276**, 779 (1997).
19. S. R. Quake, A. Scherer, *Science* **290**, 1536 (2000).
20. D. C. Duffy, J. C. McDonald, O. J. A. Schueller, G. M. Whitesides, *Anal. Chem.* **70**, 4974 (1998).
21. C. Albrecht *et al.*, *Science* **301**, 367 (2003).
22. A hand-waving argument: Upon separation, the binding energy is overcome in the shear geometry within a much shorter distance than in the unzip geometry, therefore the force to overcome the energy barrier is much lower in the unzip geometry. Because the forced unbinding of the oligomer in shear geometry is a nonequilibrium process, its unbinding force is rate-dependent. In all experiments shown here, the duplexes were loaded with a rate of 3000 pN/s.
23. G. I. Bell, *Science* **200**, 618 (1978).
24. S. B. Smith, Y. J. Cui, C. Bustamante, *Science* **271**, 795 (1996).
25. B. Essevaz-Roulet, U. Bockelmann, F. Heslot, *Proc. Natl. Acad. Sci. U.S.A.* **94**, 11935 (1997).
26. M. Rief, H. Clausen-Schaumann, H. E. Gaub, *Nat. Struct. Biol.* **6**, 346 (1999).
27. G. Neuert, C. H. Albrecht, H. E. Gaub, *Biophys. J.* **93**, 1215 (2007).
28. J. Morfill *et al.*, *Biophys. J.* **93**, 2400 (2007).
29. T. Strunz, K. Oroszlan, R. Schafer, H. J. Guntherodt, *Proc. Natl. Acad. Sci. U.S.A.* **96**, 11277 (1999).
30. R. D. Vale *et al.*, *Nature* **380**, 451 (1996).
31. G. Seisenberger *et al.*, *Science* **294**, 1929 (2001).
32. P. Tinnefeld, M. Sauer, *Angew. Chem. Int. Ed.* **44**, 2642 (2005).
33. G. Schitter *et al.*, *IEEE Trans. Control Syst. Technol.* **15**, 906 (2007).
34. P. Vettiger *et al.*, *IBM J. Res. Devel.* **44**, 323 (2000).


35. Helpful discussions with P. Hansma, G. M. Whitesides, J. Fernandez, H. Heus, P. Tinnefeld, J. Morfill, C. Albrecht, and L. Whetton are gratefully acknowledged. Supported by the German Science Foundation and the Nanosystems Initiative Munich.


### Supporting Online Material

www.sciencemag.org/cgi/content/full/319/5863/594/DC1
Materials and Methods
Figs. S1 to S5
References
Movie S1

9 October 2007; accepted 18 December 2007
10.1126/science.1151424